ACCSCIENCE PUBLISHING

Asian Journal of Water, Environment and Pollution. Vol. 22, No. 6 (2025), pp. 120-133.
doi: 10.36922/AJWEP025110078

ORIGINAL RESEARCH ARTICLE

Eco-friendly treatment of laboratory wastewater using plantain pseudo-stem

Hemalatha Kuppusamy[1]* and Ilangeswaran Dhanasamy[2]

[1]Department of Chemistry, Justice Basheer Ahmed Sayeed College for Women, Chennai, Tamil Nadu, India
[2]Department of Chemistry, Rajah Serfoji Government College, Thanjavur, Tamil Nadu, India
***Corresponding author**: Hemalatha Kuppusamy (hemalatha.k@jbascollege.edu.in)

Received: March 16, 2025; 1st revised: June 12, 2025; 2nd revised: July 15, 2025; 3rd revised: August 4, 2025; Accepted: July 25, 2025; Published online: August 28, 2025

Abstract: Chemical waste accumulates in the environment due to the improper disposal of laboratory wastewater. Wastewater generated after inorganic analysis typically contains hardness-causing substances, resulting in elevated oxygen demand. However, conventional wastewater treatment is often prohibitively expensive, especially in resource-limited settings. An eco-friendly method is therefore essential for recycling laboratory wastewater for washing purposes. In this study, laboratory wastewater was treated using a natural adsorbent—raw plantain pseudo-stem (RPPS)—and its powdered form (PPPS). Post-treatment analysis showed significant improvement in the physical and chemical parameters. Water quality indicators, such as pH, total dissolved solids (TDS), turbidity, conductivity, biological oxygen demand, chemical oxygen demand, and concentrations of heavy metals (lead, cadmium, mercury, iron, and copper), were assessed before and after treatment using inductively coupled plasma mass spectrometry. Results showed that both RPPS and PPPS were effective, eco-friendly, and cost-efficient for laboratory wastewater treatment, with PPPS exhibiting superior adsorption performance.

Keywords: Plantain pseudo-stem; Natural adsorbent; Wastewater treatment; Total dissolved solids; Biological oxygen demand; Chemical oxygen demand

1. Introduction

Water is indispensable for all living organisms. With the increasing global population, water demand is rising daily, while groundwater and surface water levels are diminishing due to excessive use.[1,2] Water treatment and reuse are widely recognized as effective solutions to address water supply challenges.[3] As water is continuously used, it becomes contaminated; thus, purification at the end of use is essential and is typically achieved through various treatment methods. It has been found that in developing countries, more than 1.6 billion people use unhygienic water, resulting in widespread incidence of diarrhea and other waterborne diseases.[4,5] Researchers have explored the use of natural materials—including fruits, vegetables, seeds, leaves, roots, and stem peels of plants—for their potential in water purification.[1,3,6-9] Various techniques have been investigated for the removal of heavy metal ions from water, including precipitation, membrane filtration, ion exchange, coagulation and flocculation, magnetic separation, biosorption, and adsorption.[10-20]

Agricultural biomass is a readily available, inexpensive, easy-to-handle, and environmentally benign material, making it a viable option for biosorption and adsorption of heavy metal ions from water.[17,18,21-25]

The banana fruit, an agricultural commodity valued at USD 63.6 billion, has a projected global production of 127.3 million tons.[22,24] India, accounting for 29% of global production, is the largest producer of bananas, followed by China and the Philippines. Notably, 60–80 tons of plantain stems per hectare are produced during fruit harvesting.[26,27] The plantain stem is the heaviest component of the banana plant, while the plantain pseudo-stem is hard, fibrous, and non-edible.[7,13,28]

In India, banana trees are integral to many auspicious rituals, particularly in South India, resulting in the widespread availability of plantain pseudo-stems. Once the fruit ripens and is harvested, the pseudo-stem—no longer functional—is chopped and often converted into waste biomass. While plantain stems are utilized for their therapeutic properties, the pseudo-stem is typically discarded.[29-31] Both the pseudo-stem and the stem play a crucial role in the transport of nutrients from the soil to the fruit. After harvest, the banana plant ceases to be useful, and the pseudo-stems are often burned or disposed of in rivers and lakes.[32,33]

Due to their high cellulose content and hygroscopic properties, banana stems are effective as a porous medium.[34] The stem filter media is capable of significantly lowering chemical oxygen demand (COD), total suspended solids levels, and turbidity during wastewater treatment processes.[35,36] Furthermore, chemical pre-treatments can reduce energy usage by improving the fibrillation of cellulose materials, altering the adsorbent surface, and boosting its capacity for ion adsorption.[22,37-39]

Chemicals used in laboratories are often disposed of as waste. However, improper disposal practices result in the discharge of water with persistence of hardness and other contaminants, leading to high oxygen demand, heavy metal accumulation, and environmental pollution. The high cost of wastewater treatment, especially under resource constraints, poses a significant challenge. This study examines the use of accessible and cost-effective pseudo-stems as a potential adsorbent for the purification of laboratory wastewater.

2. Materials and methods

2.1. Materials

The pseudo-stems were sourced from local vegetable markets in Chennai, India. The raw pseudo-stems were thoroughly cleaned with distilled water to remove dirt and debris, and then chopped into small fragments.

These fragments were oven-dried at 120°C for 4 h, ground using a high-speed grinder, and sieved through a 100-micron mesh to obtain uniform powdered material. For chemical activation, the pseudo-stem powder was treated with 5% acetic acid (Sigma-Aldrich, India) at 60°C for 2 h to enhance its porosity and surface area (Figure 1).

Laboratory wastewater was collected using sterile 5 L polyethene containers (Tarsons, India) placed beneath a laboratory sink during peak usage hours. Composite samples were obtained over a 3-h period to account for variability in discharge. The collected samples were immediately stored at 4°C and analyzed within 24 h.

2.2. Laboratory wastewater treatment with raw plantain pseudo-stem (RPPS)

Chopped RPPS was added at a concentration of 50 g/L to inert glass containers (Borosil, India), each containing 1 L aliquots of the untreated laboratory wastewater samples (S1–S5), Table 1. Each mixture was left undisturbed for 24 h at room temperature (25 ± 2°C). No pH adjustment was performed, and natural pH (5.5–6.8) was retained to reflect real laboratory conditions.

After treatment, the supernatant was decanted and filtered, yielding first-stage filtrate, referred to as F1. This process was repeated using fresh RPPS for up to four treatment cycles, producing sequential filtrates F2 through F4. F2–F3 are considered intermediate-stage treated water, while F4 is the final-stage treated water.

For each stage, the following parameters were measured: pH, TDS, turbidity, conductivity, COD, biological oxygen demand 5 days (BOD_5), and metal concentrations (lead, cadmium, mercury, iron, and copper). Digital pH meters (Systronics,

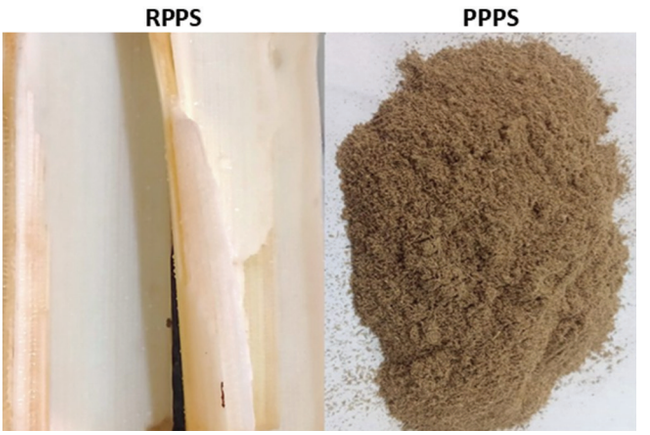

Figure 1. Photos of raw and powdered plantain pseudo-stem (RPPS and PPPS)

Table 1. Characteristics of laboratory wastewater samples

Sample	Metal	pH	TDS (mg/L)	COD (mg/L)	BOD_5 (mg/L)	Conductivity (mS/cm)	Turbidity (NTU)
S1	Lead	6.8	1660	42.6	5.4	2.4	27.0
S2	Cadmium	6.6	1750	56.0	4.8	2.6	22.2
S3	Mercury	5.5	1520	60.8	4.7	2.2	45.0
S4	Iron	5.8	1620	48.5	8.0	2.4	30.8
S5	Copper	6.0	1820	50.6	6.2	2.6	40.8

Abbreviations: BOD_5: Biological oxygen demand (5 days); COD: Chemical oxygen demand; mS/cm: milliSiemens per centimeter; NTU: Nephelometric turbidity unit; TDS: Total dissolved solids.

India), conductivity meters (Systronics, India), and TDS meters (Eutech Instruments, Singapore) were used. Turbidity was measured with a nephelometer (HACH 2100Q, USA; supplied in India). COD and BOD_5 were analyzed according to the standard methods provided by the American Public Health Association (APHA) for the examination of water and wastewater. Metal concentrations were determined using inductively coupled plasma mass spectrometry (Agilent 7900, USA). Fourier transform infrared spectroscopy (FTIR) analysis (PerkinElmer Spectrum Two, USA) was conducted. Scanning electron microscopy (SEM) analysis (Carl Zeiss, India) was conducted. All treatments were conducted in triplicate (n = 3), and the results are reported as mean ± standard deviation.

2.3. Laboratory wastewater treatment with chemically activated powdered plantain pseudo-stem (PPPS)

One gram of PPPS was added to 1 L screw-capped conical flasks (Borosil, India) containing the wastewater samples (S1–S5). The mixture was left for 24 h at room temperature (25 ± 2°C) under natural pH conditions (5.5–6.8). After settling, the mixture was filtered to obtain filtrate-1 (F1). This was then subjected to a second round of treatment with fresh PPPS (1 g), yielding filtrate-2 (F2).

All physicochemical parameters and heavy metal concentrations were analyzed for both raw and treated samples, following the same protocols and instrumentation as in the RPPS treatment.

A blank control (PPPS and distilled water) and a negative control (wastewater without PPPS) were processed alongside experimental samples to confirm treatment-specific effects.

2.4. Derivation of adsorption parameters

The experimental data in Table 2 were used to derive parameters for adsorption isotherm modeling. The amount of lead ions (Pb^{2+}) adsorbed at equilibrium (qe, mg/g) was calculated using the mass balance equation (Equation I):

$$qe = \frac{(Cs - Ce) \times V}{m} \quad \text{(I)}$$

Where Cs is the initial concentration of Pb^{2+} (fixed at 150 mg/L),

Ce is the equilibrium concentration (mg/L),

V is the volume of the solution (L),

and m is the mass of the adsorbent (g).

The derived parameters include: (1) Ce/qe for linearized Langmuir isotherm fitting; (2) ln(Ce) and ln(qe) for Freundlich isotherm fitting; and Ce/(Cs − Ce) and Ce/[(Cs − Ce) × qe] for Brunauer-Emmett-Teller (BET) isotherm analysis.

All logarithmic values are natural logarithms. These transformations enable direct comparison with the respective linear forms of the adsorption models and were applied uniformly across all experimental data.

2.5. Statistical analysis

Statistical analysis was performed using one-way analysis of variance to assess significant differences between treatment groups, with a significance threshold set at p<0.05. All analyses were carried out using ORIGIN 8 Pro software (OriginLab Corporation, USA).

2.6. Recovery of PPPS

Following biosorption, the PPPS underwent a recovery process to evaluate its potential for reuse in multiple adsorption cycles. The spent biosorbent was treated with 0.1 M hydrochloric acid, using a solid-to-liquid ratio of 1 g powder to 30 mL of eluent. The suspension was shaken for 60 min to facilitate desorption of the metal ions, after which it was separated by filtration.[40] The recovered biosorbent was thoroughly washed with distilled water to remove acid residues and then dried in a hot air oven at 120°C for 2 h.

Table 2. Experimental and calculated parameters for adsorption isotherm modeling

Ce (mg/L)	qe (mg/g)	Ce/qe	ln (Ce)	ln (qe)	Cs−Ce	Ce/(Cs−Ce)	Ce/([Cs−Ce]×qe)
10	1.2	8.33	2.30	5.30	140	0.0714	0.0595
20	2.0	10.00	3.00	6.90	130	0.1538	0.0769
40	3.0	13.33	3.69	8.50	110	0.3636	0.1212
60	3.6	16.67	4.10	9.43	90	0.6667	0.1852
80	4.0	20.00	4.38	10.09	70	1.1429	0.2857
100	4.2	23.81	4.61	10.61	50	2.0000	0.4762

Notes: All calculations assume a constant initial concentration of Cs=150 mg/L. Derived parameters were computed for the linearization of Langmuir, Freundlich, and BET isotherm models.
Abbreviations: BET: Brunauer–Emmett–Teller; Ce: Equilibrium concentration; Cs: Initial concentration; qe: Amount adsorbed at equilibrium.

3. Results and discussion

Before assessing the effectiveness of RPPS and PPPS in treating laboratory wastewater, control samples were examined. The blank controls (distilled water with RPPS or PPPS) showed minimal changes across all measured parameters, confirming that the adsorbents alone did not release significant contaminants or interfere with the readings. In the negative controls (untreated wastewater maintained under identical conditions), no notable changes in pH, TDS, turbidity, BOD_5, COD, or metal concentrations were observed after 24 h. These findings indicate that passive settling or environmental factors did not significantly contribute to parameter reductions, confirming that the improvements observed in treated samples were specifically attributable to RPPS and PPPS.

3.1. Physical characteristics of water samples

The untreated wastewater samples exhibited strong turbidity, dark coloration, and unpleasant odor, indicative of high pollutant load. In contrast, water treated with RPPS and PPPS showed noticeable improvement in color, clarity, and odor. These qualitative changes suggest effective removal or reduction of both organic and inorganic contaminants.

3.2. Variation in physicochemical parameters

Significant improvements in physicochemical parameters were observed post-treatment. Figures 2-4 display the comparative data for untreated and treated water across both RPPS and PPPS treatments.

Laboratory analysis showed consistent improvements in water quality after treatment. The pH values stabilized within the optimal range (6.0–7.5), and the acidic samples showed an increase in pH39. Alkaline samples exhibited a slight decrease in pH, indicating the buffering action of the biosorbent (Figures 2A and 3A). Significant reductions were observed in TDS, electrical conductivity (Figures 2B-C and 3B-C), and turbidity (70–90%) (Figures 2D and 3D), indicating efficient deionization and removal of suspended particulates. In addition, both COD and BOD_5 markedly decreased (Figures 2E-F and 3E-F), pointing to substantial removal of organic matter and microbial load.[35] Heavy metal removal exceeded 90% for lead, cadmium, mercury, iron, and copper, with PPPS demonstrating slightly better performance than RPPS (Figure 4).

3.3. FTIR analysis

3.3.1. FTIR analysis of PPPS

FTIR spectrum of PPPS (Figure 5) revealed characteristic peaks associated with cellulose (1026, 1423, and 891 cm^{-1}), lignin (1511 and 1635 cm^{-1}), and hemicellulose esters and acetyl groups (1736 cm^{-1}). Strong hydroxyl group absorption at 3417 cm^{-1}, important for adsorption processes, was also observed, along with peaks at 2920 cm^{-1} and 2850 cm^{-1}, corresponding to aliphatic groups, likely representing waxes or lipophilic substances.

3.3.2. FTIR analysis of Pb^{2+}-adsorbed PPPS

The FTIR analysis of Pb^{2+}-adsorbed PPPS (Figure 6) confirmed that adsorption occurs through complexation with hydroxyl and carboxyl groups, interaction with lignin/aromatic and alcohol sites, and structural modifications reflected by shifts and suppression of key absorption bands (Table 3).

3.4. Batch adsorption study

A batch adsorption experiment was conducted to assess the efficacy of pre-treated plantain pseudo-stem as a biosorbent for removing Pb^{2+} from aqueous solutions. The system was maintained under controlled conditions using a constant volume of 100 mL and a

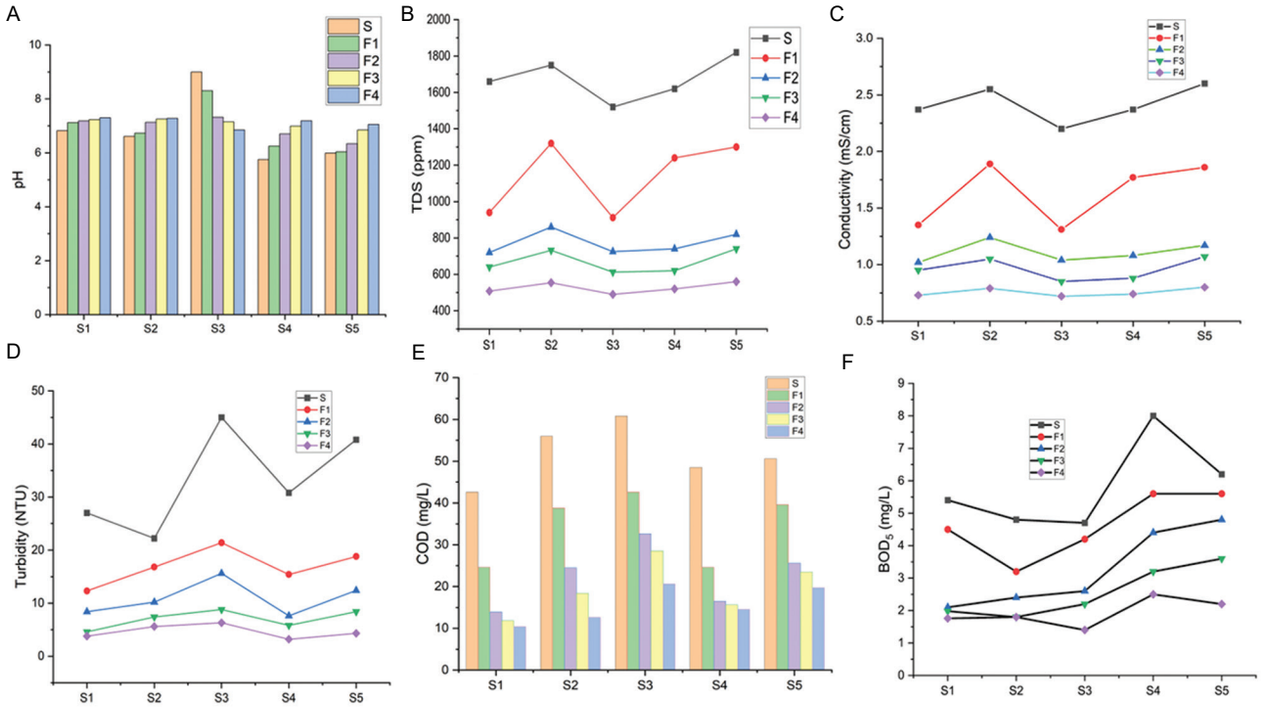

Figure 2. Variation of pH, TDS, electrical conductivity, turbidity, COD, and BOD_5 in the water samples treated with RPPS. Five wastewater samples (S1–S5) were untreated (S) or subjected to multiple rounds of RPPS treatment (F1–F4)

Abbreviations: BOD_5: Biological oxygen demand (5 days); COD: Chemical oxygen demand; mS/cm: millisiemens per centimetre; NTU: Nephelometric turbidity unit; RPPS: Raw plantain pseudo-stem; TDS: Total dissolved solids

Table 3. FTIR analysis of PPPS before and after adsorption of Pb^{2+}

Wavenumber (cm^{-1})	Peak (unadsorbed)	Peak (Pb^{2+} adsorbed)	Functional group	Interpretation
~3417	3417.53	3416.13	O–H stretching	Slight shift of H-bonding affected by Pb^{2+} interaction with hydroxyl groups
~2920	2920.10	2923.82	C–H (aliphatic)	Minor shift, possibly due to structural reordering
~1736	1736.28	Absent	C=O (carbonyl)	Disappearance suggests Pb^{2+} complexation with carboxyl groups in hemicellulose
~1635	1635.45	1636.24	Aromatic C=C/H_2O	Unchanged lignin/aromatic region
~1511	1511.37	Absent	Lignin (C=C)	Disappearance may indicate Pb^{2+} interaction with aromatic rings
~1423	1423.84	1435.50	CH_2 bending	Slight shift due to structural rearrangement
~1247	1247.64	1249.03	C–O–C (ether)	Retained, suggesting minimal effect
~1026	1026.76	1033.26	C–O stretching	Shifted indicates interaction between Pb^{2+} and alcohol/ether groups
~891	891.63	894.20	β-glycosidic bonds	Retained, indicating cellulose backbone stability

Abbreviations: FTIR: Fourier transform infrared spectroscopy; Pb: Lead; PPPS: Powdered plantain pseudo-stem.

fixed adsorbent dosage of 2 g, resulting in a working concentration of 20 g/L. The initial Pb^{2+} concentration was set at 150 mg/L to simulate moderate contamination levels. The pH of the solution was adjusted and maintained within the optimal range of 4.5–5.5, where maximum adsorption is anticipated due to the favorable

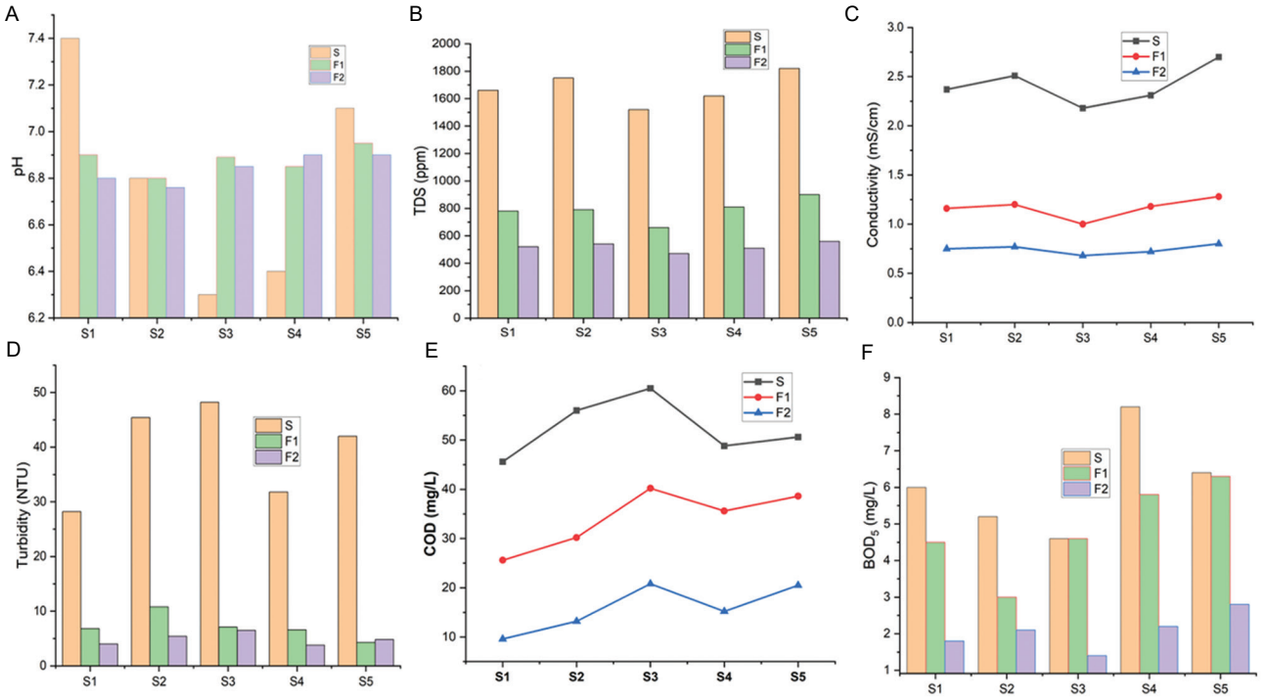

Figure 3. Variation of pH, TDS, electrical conductivity, turbidity, COD, and BOD_5 in the water samples treated with PPPS. Five wastewater samples (S1–S5) were untreated (S) or subjected to multiple rounds of PPPS treatment (F1–F2)

Abbreviations: BOD_5: Biological oxygen demand (5 days); COD: Chemical oxygen demand; mS/cm: millisiemens per centimetre; NTU: Nephelometric turbidity unit; PPPS: Powdered plantain pseudo-stem; TDS: Total dissolved solids

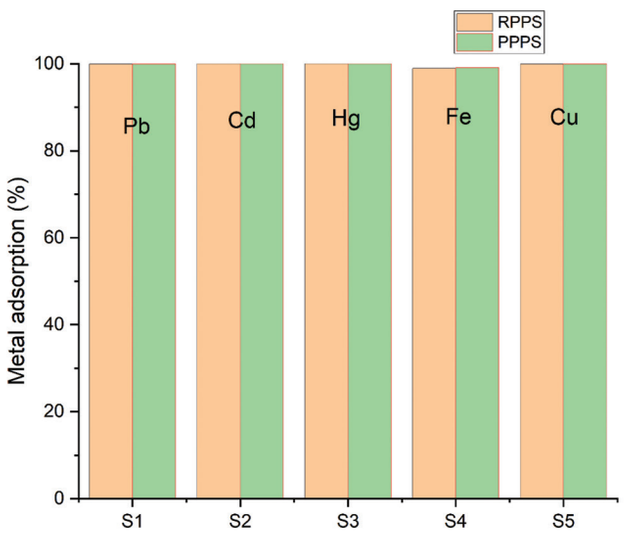

Figure 4. Percentage of metal adsorption in the water samples (S1–S5) treated with RPPS and PPPS Abbreviations: Cd: Cadmium; Cu: Copper; Fe: Iron; Hg: Mercury; Pb: Lead; PPPS: Powdered plantain pseudo-stem; RPPS: Raw plantain pseudo-stem

ionization of active surface functional groups. The temperature during the study was kept constant between 25°C and 30°C to replicate typical ambient conditions. Contact time was varied from 0 to 180 min at 30-min intervals to monitor adsorption kinetics. Samples were collected at each time point and analyzed for residual Pb^{2+} concentrations. This experimental setup facilitated the evaluation of adsorption capacity, equilibrium time, and overall performance of the plantain pseudo-stem adsorbent, providing a foundation for kinetic and isotherm modeling.[41]

3.4.1. Langmuir adsorption isotherm

The adsorption data were analyzed using the Langmuir isotherm model to evaluate the monolayer adsorption capacity and the surface affinity of the adsorbent for Pb^{2+}. The linearized form of the Langmuir equation is shown in Equation II.

$$\frac{1}{qe} = \frac{1}{q_{max}.KL}.\left(\frac{1}{Ce}\right) + \frac{1}{q_{max}} \quad \text{(II)}$$

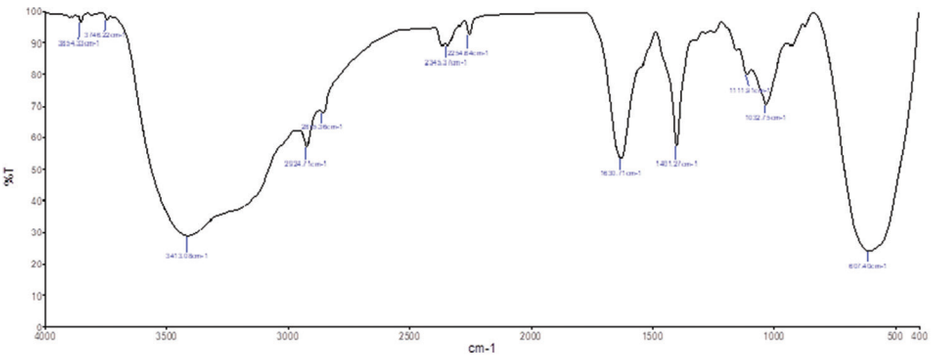

Figure 5. FTIR spectrum of PPPS
Abbreviations: FTIR: Fourier transform infrared spectroscopy; PPPS: Powdered plantain pseudo-stem

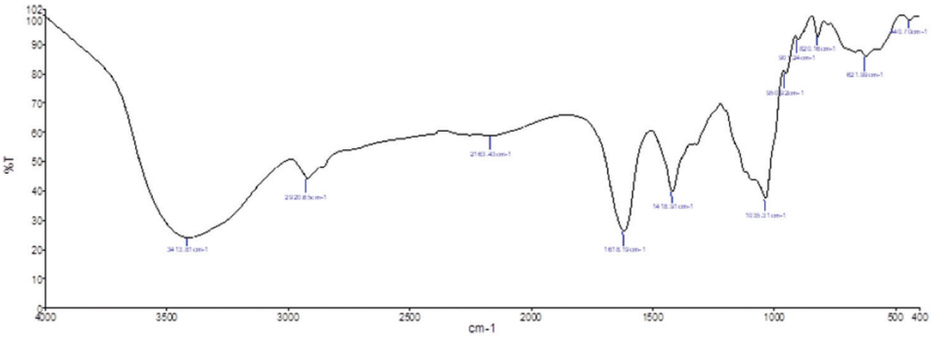

Figure 6. FTIR spectrum of Pb^{2+}-adsorbed PPPS
Abbreviations: FTIR: Fourier transform infrared spectroscopy; Pb: Lead; PPPS: Powdered plantain pseudo-stem

Where, qe = Amount of adsorbate adsorbed at equilibrium (mg/g)

q_{max} = Maximum monolayer adsorption capacity (mg/g)

KL = Langmuir adsorption constant related to the affinity of the binding sites (L/mg)

Ce = Equilibrium concentration of adsorbate in solution (mg/L).

A plot of 1/qe versus 1/Ce (Figure 7) yielded a straight line with an excellent linear fit ($R^2 = 0.99994$). The slope and intercept of the linear regression were 6.62334 and 0.17019, respectively. From these values, the Langmuir constants were calculated as follows: (1) the monolayer adsorption capacity (q_{max} = 1/ intercept) was 5.876 mg/g. (2) The Langmuir constant (KL = Slope/intercept) was 38.93 L/mg. The high q_{max} indicates that the adsorbent possesses a substantial number of active sites capable of binding the target ion. In contrast, the large value of KL reflects a strong affinity between the adsorbate and the surface. The near-unity R^2 value confirms that the adsorption process adheres to the Langmuir model exceptionally well, suggesting that adsorption occurs as a monolayer on a homogeneous surface with uniform energies of adsorption. No significant interactions between

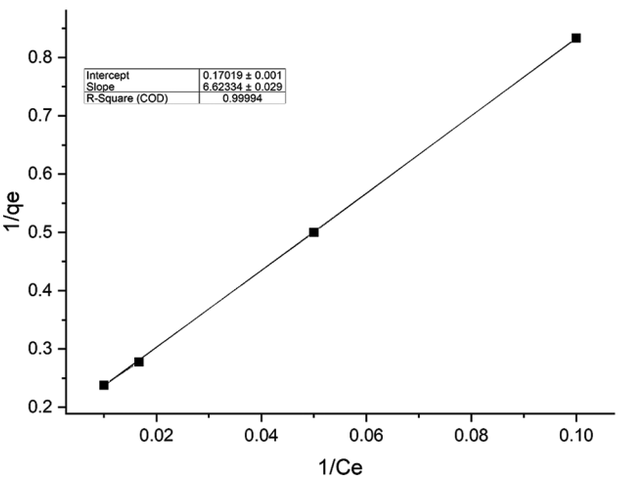

Figure 7. Langmuir isotherm modeling of Pb^{2+} adsorption by PPPS
Abbreviations: Ce: Equilibrium concentration; qe: Amount adsorbed at equilibrium; Pb: Lead; PPPS: Powdered plantain pseudo-stem

adsorbed molecules were observed, further supporting the validity of the Langmuir assumptions.

3.4.2. Freundlich adsorption isotherm

The experimental adsorption data were also evaluated using the Freundlich isotherm, an empirical model describing adsorption on heterogeneous surfaces. The linearized form of the Freundlich equation is given in Equation III.

$$\ln q_e = \ln K_F + \frac{1}{n} \ln Ce \quad \text{(III)}$$

where, qe = Amount of adsorbate adsorbed at equilibrium (mg/g)

KF= Freundlich adsorption constant indicative of adsorption capacity ([mg/g][L/mg]$^{1/n}$)

n = Freundlich intensity parameter related to adsorption favorability (dimensionless)

Ce = Equilibrium concentration of adsorbate in solution (mg/L).

A plot of ln qe versus ln Ce (Figure 8) yielded a perfectly linear relationship (R^2 = 1.000), indicating an excellent fit to the Freundlich model. The slope of the plot was 2.303, corresponding to 1/n, which represents the adsorption intensity. Thus, the Freundlich constant (n = 1/2.303) is 0.434, suggesting a chemically favorable adsorption process, as n <1 typically reflects strong interactions between adsorbate and adsorbent. The pronounced linearity of the Freundlich plot indicates that adsorption likely takes place on a heterogeneous surface with sites of varying energies and supports the presence of multilayer adsorption. In addition, the model's strong fit demonstrates that the adsorbent is effective across a wide range of adsorbate concentrations. Overall, the Freundlich isotherm accurately characterizes the adsorption behavior, and the high slope value indicates strong affinity and a non-uniform energy distribution among adsorption sites.

3.4.3. BET adsorption isotherm

The linearized BET equation is given in Equation IV.

$$\frac{Ce}{(Cs - Ce)qe} = \frac{1}{qm.C} + \frac{C-1}{qm.C}.\left(\frac{Ce}{Cs}\right) \quad \text{(IV)}$$

Where, Ce = Equilibrium concentration of adsorbate in solution (mg/L)

Cs = Initial adsorbate concentration in the solid phase (mg/L)

qe = Amount of adsorbate adsorbed at equilibrium (mg/g)

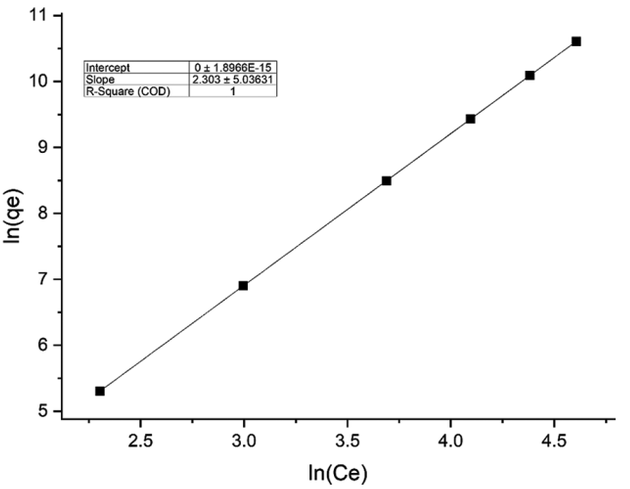

Figure 8. Freundlich isotherm modeling of Pb^{2+} adsorption by PPPS

Abbreviations: Ce: Equilibrium concentration; Cs: Initial concentration; qe: Amount adsorbed at equilibrium; Pb: Lead; PPPS: Powdered plantain pseudo-stem

qm = Maximum monolayer adsorption capacity (mg/g)

C = Dimensionless constant related to adsorption affinity.

A plot of Ce/(Cs−Ce) versus Ce/([Cs−Ce] qe) (Figure 9) yielded a highly linear trend (R^2 = 0.99983), indicating excellent agreement between the experimental data and the BET model. The slope and intercept were obtained as 0.21563 and 0.04268, respectively. Using these values, the BET constants were calculated: (1) Monolayer adsorption capacity (qm = 1/[slope + intercept]) is 3.98 mg/g; and (2) BET constant (C = 1 + [slope/intercept]) is 6.05.

These results indicate that multilayer adsorption plays a significant role and that the adsorbent has a well-defined surface with moderate affinity for Pb^{2+} beyond monolayer coverage. The high C value suggests favorable adsorbate–adsorbent interactions in the first adsorption layer, which is a key feature of BET-type behavior.

Overall, the adsorption data suggest that the monolayer plateau begins near a qe value of 4.2 mg/g, indicating a good fit for the Langmuir isotherm, which assumes monolayer adsorption on a homogeneous surface. However, the non-linear and increasing qe values at higher concentrations suggest a better fit with the Freundlich isotherm, which accounts for heterogeneous surface energies and multilayer adsorption behavior.

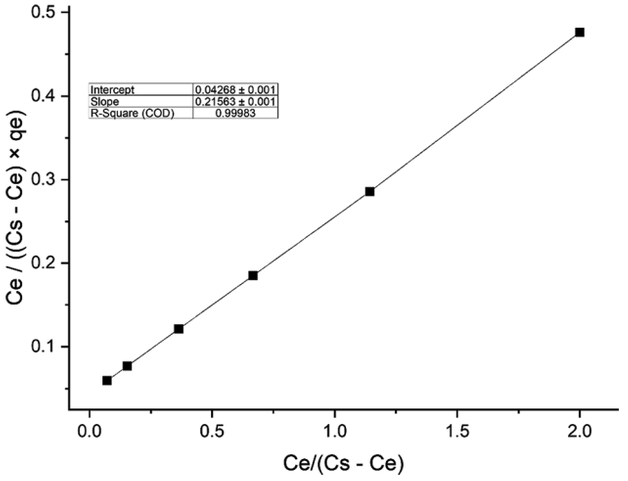

Figure 9. BET isotherm modeling of Pb^{2+} adsorption by PPPS

Abbreviations: BET: Brunauer–Emmett–Teller; Ce: Equilibrium concentration; qe: Amount adsorbed at equilibrium; Pb: Lead; PPPS: Powdered plantain pseudo-stem

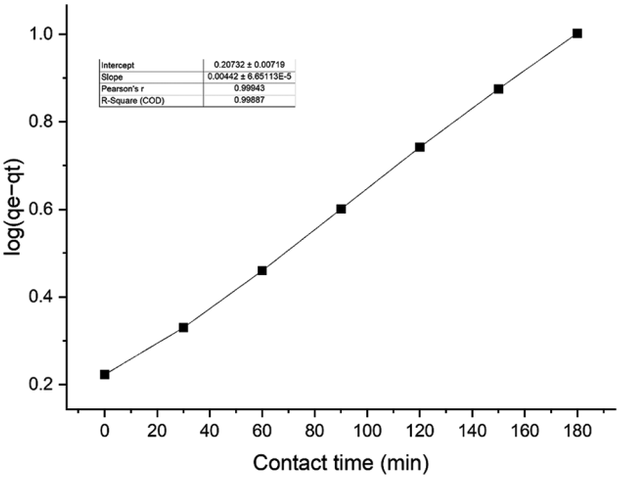

Figure 10. Pseudo-first-order kinetic model for the adsorption of Pb^{2+} by PPPS

Abbreviations: qe: Amount adsorbed at equilibrium; qt: Amount of adsorbate adsorbed at time t; Pb: Lead; PPPS: Powdered plantain pseudo-stem

Moreover, the trend beyond 80 mg/L shows signs of additional adsorption layers forming, which supports the applicability of the BET model for multilayer adsorption at higher concentrations.

3.5. Adsorption kinetics

Kinetic studies are crucial for understanding the adsorption mechanism and rate-controlling steps, which aid in optimizing adsorption processes. Among the commonly used models, the pseudo-first-order model typically describes physisorption, while the pseudo-second-order model is often associated with chemisorption as the rate-limiting step. Comparing model parameters and correlation coefficients helps identify the best-fitting mechanism and provides insights into the adsorbate–adsorbent interaction and system efficiency.

3.5.1. Pseudo-first-order

The adsorption kinetics were evaluated using the pseudo-first-order model. A linear plot of Figure 10 showed excellent correlation ($R^2 = 0.99887$), indicating good agreement with the model. The rate constant (k1) was calculated from the slope ($0.00442 \pm 6.65 \times 10^{-5}$), and the intercept ($0.20732 \pm 0.00719$) corresponds to log(qe). The high Pearson's correlation coefficient ($R = 0.99943$) and the low residual sum of squares (5.57×10^{-4}) confirm that the adsorption follows pseudo-first-order kinetics under the studied conditions.[41]

3.5.2. Pseudo-second-order

The adsorption kinetics were further evaluated using the pseudo-second-order model, which is based on the assumption that the adsorption process may involve chemisorption through electron sharing or exchange between the adsorbent and adsorbate. A linear plot of t/qt versus time (Figure 11) yielded a high correlation coefficient ($R^2 = 0.99023$), indicating that the experimental data fit the model well. The slope and intercept of the plot were 0.2294 ± 0.01019 and 2.42643 ± 1.10253, respectively, from which the equilibrium adsorption capacity and the pseudo-second-order rate constant were determined. The high Pearson's R value (0.9951) and the relatively low residual sum of squares (13.09) further support the applicability of this model.[41] These results suggest that the adsorption process follows pseudo-second-order kinetics, implying that chemisorption is likely the rate-limiting step. Overall, the model provides a good description of the experimental data and indicates a strong interaction between the adsorbate and adsorbent.

3.6. Comparative performance: RPPS versus PPPS

A comparative assessment between RPPS and PPPS treatments revealed that PPPS achieved equal or superior contaminant removal using only two treatment cycles, compared to five cycles required for RPPS. The enhanced efficiency of PPPS is attributed to its greater surface area, fibrous structure, and porous morphology, which collectively increase the number of active adsorption sites.

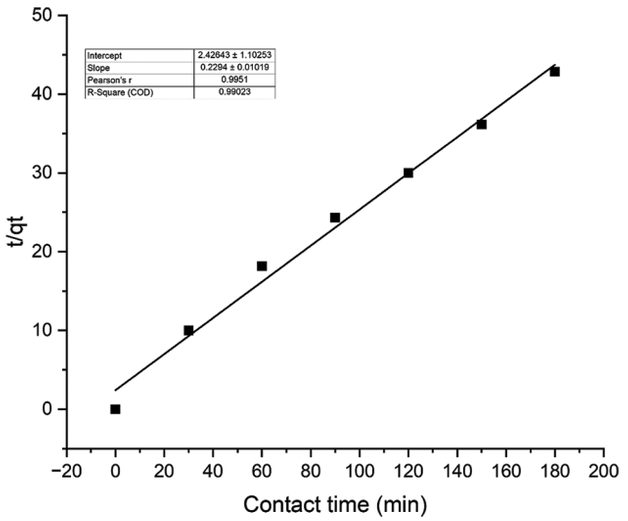

Figure 11. Pseudo-second-order kinetic model for the adsorption of Pb^{2+} by PPPS

Abbreviations: qe: Amount adsorbed at equilibrium; qt: Amount of adsorbate adsorbed at time t; Pb: Lead; PPPS: Powdered plantain pseudo-stem

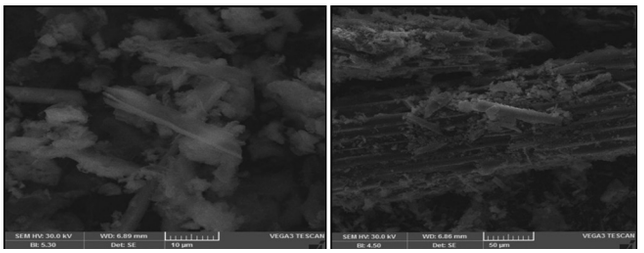

Figure 12. SEM images of PPPS

Abbreviations: SEM: Scanning electron microscopy; PPPS: Powdered plantain pseudo-stem

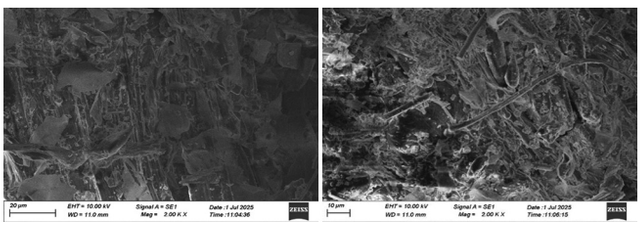

Figure 13. SEM images of the Pb^{2+} adsorbed PPPS

Abbreviations: SEM: Scanning electron microscopy; Pb: Lead; PPPS: Powdered plantain pseudo-stem

3.6.1. Morphological analysis and adsorption potential of PPPS

The SEM analysis (Figure 12) of PPPS reveals a rough, porous surface interspersed with fibrous structures, significantly increasing its active surface area. This structural characteristic is advantageous for adsorption applications, as the increased surface exposure provides a greater number of binding sites for metal ions, thereby improving adsorption capacity.

Furthermore, the observed variation in particle size and shape may contribute to non-uniform binding efficiency across different regions of the material. However, the overall adsorption potential remains high due to the presence of extensive surface structures available for interaction. Notably, the presence of elongated fibrous structures, likely representing lignocellulosic bundles, suggests incomplete delignification, particularly if the material underwent pre-treatment for fiber extraction. Residual lignin and hemicellulose could influence the surface chemistry and metal ion affinity, highlighting the need for further investigation into their role in adsorption efficiency.

3.6.2. SEM analysis of Pb^{2+}-adsorbed PPPS

After exposure to Pb^{2+} ions, the surface undergoes a notable morphological transformation as shown in Figure 13. The previously defined fibrous structure appears distorted and irregular, with amorphous and granular deposits visible on the surface. These particulates are likely lead complexes or precipitates, formed as Pb^{2+} interacts with functional groups on the plant matrix. Increased roughness, pore formation, and fiber fragmentation are also evident, indicating that metal ion binding may have caused localized swelling, collapse, or chemical etching of the biomass surface. These changes suggest the formation of surface complexes between Pb^{2+} ions and oxygen-containing functional groups.

These morphological changes strongly support the hypothesis that Pb^{2+} adsorption on plantain pseudo-stem occurs through a combination of surface complexation and ion-exchange, facilitated by the natural porosity and functional groups in the biomass. The post-adsorption surface damage and particle deposition are clear indications of successful metal uptake. These findings, when combined with FTIR results, suggest that hydroxyl, carbonyl, and ether groups play a significant role in metal binding. This underscores the adsorptive potential of plantain pseudo-stem for heavy metal removal from aqueous systems.

3.6.3. SEM analysis of recovered PPPS

The surface morphology of the recovered plantain pseudo-stem (Figure 14) reveals a noticeably more porous and rough texture, resulting from the degradation of hemicellulose and partial delignification during the treatment process. These structural alterations are

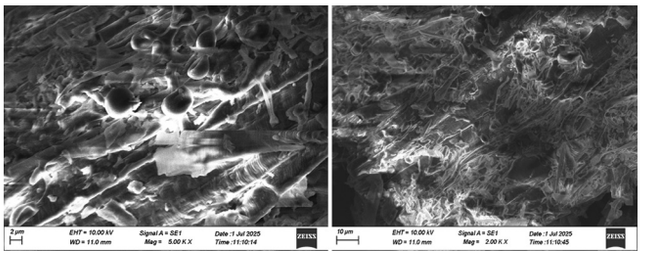

Figure 14. SEM images of the recovered PPPS
Abbreviations: SEM: Scanning electron microscopy; PPPS: Powdered plantain pseudo-stem

accompanied by visible cracks, micro fissures, and loosened fiber bundles, which collectively contribute to an increased surface area—an advantageous feature for subsequent adsorption-based applications. Disruption at the cell wall level is also evident, with signs of rupture and swelling, particularly in samples subjected to microbial or chemical hydrolysis, indicating active biodegradation on the surface. In addition, the presence of granular or crystalline deposits suggests residual salts or precipitates from wastewater exposure. Compared to untreated material, the treated pseudo-stem appears cleaner but more fragmented, with a clearer delineation of fiber bundles due to the separation of the supporting matrix. These changes demonstrate the enhanced suitability of the processed pseudo-stem for further functionalization or use in value-added applications, such as biosorption, composite development, or enzymatic hydrolysis.

3.7. Reusability of PPPS

The regeneration efficiency of PPPS was assessed over three consecutive cycles. The first cycle maintained high removal of Pb^{2+}, while the second and third cycles retained approximately 75% and 50% of the initial adsorption capacity, respectively. The sustained performance in later cycles is attributed to the acid treatment's ability to restore a significant proportion of active sites by desorbing bound Pb^{2+} ions, while preserving the structural integrity of the biomass. A gradual decline in capacity likely results from irreversible binding, structural degradation, or partial loss of functional groups during repeated use.

3.8. Comparative performance of PPPS with other biosorbents

As reported in Section 3.4.1, the monolayer adsorption capacity of PPPS for Pb^{2+} was approximately 5.88 mg/g. When compared with other agricultural biosorbents, such as banana peel (3.6–5.1 mg/g),[42] orange peel (4.8–6.2 mg/g),[43] and sugarcane bagasse (4.5–7.4 mg/g),[44] PPPS demonstrates competitive performance. This highlights its effectiveness and suitability as a low-cost, high-potential biosorbent. Furthermore, unlike many biosorbents that require extensive chemical pre-treatment, PPPS performed well with minimal processing, making it more accessible and environmentally favorable for real-world applications.

3.9. Applicability and environmental impacts

Although the chemical parameters of the treated water did not fully meet the drinking water standards set by Indian regulatory agencies, biosorption with plantain pseudo-stem significantly improved water quality. Parameters, such as pH, TDS, COD, BOD_5, and heavy metal concentrations were notably reduced, making the treated water suitable for non-potable applications, such as laboratory washing and industrial reuse. This has meaningful implications for water conservation in resource-limited settings, where potable water must be preserved for essential uses. The study suggests that while the biosorbent may not yet replace conventional purification technologies for potable water, it offers a promising, cost-effective solution for secondary water treatment.

The study highlights the simplicity and cost-effectiveness of the plantain pseudo-stem in the purification process. A container is sufficient for PPPS and RPPS methods, requiring minimal infrastructure and equipment. Furthermore, plantain pseudo-stems are commonly available waste biomass, making them an attractive choice for utilization as a biosorbent. This makes the purification process environmentally friendly and sustainable, as it utilizes a renewable and abundant resource.

The observed fungal growth on the plantain pseudo-stem after RPPS treatment indicates that it undergoes degradation easily. The demonstrated reusability of PPPS further enhances the sustainability of the purification process by reducing waste generation and resource consumption.

4. Conclusion

The increasing discharge of laboratory wastewater, laden with chemical residues, poses a significant challenge to environmental sustainability. Given the indispensable role of chemicals in scientific research, particularly in the field of chemistry, there is a pressing need for environmentally responsible treatment strategies that do not compromise the integrity of research.

In this study, we experimentally demonstrated a sustainable and efficient approach to laboratory wastewater treatment using plantain pseudo-stem, an abundant agricultural by-product in India, traditionally discarded after ceremonial use. Both raw and powdered samples were evaluated as biosorbents. The findings reveal substantial improvements in water quality, including significant reductions in pH imbalance, turbidity, TDS, electrical conductivity, BOD_5, COD, and heavy metal concentrations. Notably, PPPS exhibited enhanced adsorption capacity with fewer treatment cycles, due to its higher surface area and porous morphology.

Beyond its technical efficacy, this biosorbent offers broader environmental benefits. Treated water, although not potable, meets the quality criteria for secondary applications, such as laboratory washing, thereby reducing freshwater dependency. Furthermore, the spent biosorbent, being biodegradable, can be repurposed as compost, closing the loop within a circular waste management framework.

This work underscores the viability of plantain pseudo-stem as a cost-effective, eco-friendly biosorbent for decentralized wastewater treatment in academic and research laboratories. Its implementation supports not only environmental conservation but also promotes the utilization of agro-waste in practical, scalable applications. Looking forward, the development of filtration units or column-based systems incorporating PPPS could enable continuous flow treatment, further extending its utility in real-world settings. Integrating such bio-based solutions into laboratory infrastructure represents a meaningful advancement in the pursuit of green chemistry and sustainable research practices.

Acknowledgments

The authors are grateful to the Chemistry department, Microbiology department, and Multi-Disciplinary Research and Consultancy Centre (MRCC) of Justice Basheer Ahmed Sayeed College for Women for providing instrument facilities.

Funding

This work was partially supported by the MRCC of Justice Basheer Ahmed Sayeed College for Women, Chennai.

Conflict of interest

The authors declare no competing interests.

Author contributions

Conceptualization: All authors
Investigation: Hemalatha Kuppusamy
Methodology: Hemalatha Kuppusamy
Formal analysis: All authors
Writing – original draft: Hemalatha Kuppusamy
Writing – review & editing: All authors

Availability of data

Data are available from the corresponding author upon reasonable request.

Further disclosure

Part of the findings have been presented in an international conference on "Frontiers of Sustainable Research in Healthcare, Food, Agriculture and Environment Management" (ICSURE-2024), organized by Guru Nanak College, Chennai.

References

1. Demirbas A. Heavy metal adsorption onto agro-based waste materials: A review. *J Hazard Mater*. 2008;157(2-3):220-229.
doi: 10.1016/j.jhazmat.2008.01.024
2. Gaber MM, Samy M, Shokry H. Effective degradation of synthetic micropollutants and real textile wastewater via a visible light-activated persulfate system using novel spinach leaf-derived biochar. *Environ Sci Pollut Res*. 2024;31:25163-25181.
doi: 10.1007/s11356-024-32829-6
3. Pathak PD, Mandavgane SA, Kulkarni BD. Fruit peel waste as a novel low-cost bio adsorbent. *Rev Chem Eng*. 2015;31(4):361-381.
doi: 10.1515/revce-2014-0041
4. Naragundkar NS, Kavya BK, Manoj Kumar KS, Ganga MM, Manoj SK. *Industrial Waste Water Tretment Using Banana Stem Extract* [Easy Chair Preprint]; 2022.
5. Ferronato N, Paoli R, Romagnoli F, Tettamanti G, Bruno D, Torretta V. Environmental impact scenarios of organic fraction municipal solid waste treatment with black soldier fly larvae based on a life cycle assessment. *Environ Sci Pollut Res*. 2024;31(12):17651-17669.
doi: 10.1007/s11356-023-27140-9

6. El-Maghraby A, Taha NA, Mahmoud A, El-Aziz A. Preparation of activated carbon (chemically and physically) from banana pith for heavy metal removal from wastewater. *Sci-Afric J Sci Issues Res Essays*. 2014;2:399-403.
7. Kokate S, Parasuraman K, Prakash H. Adsorptive removal of lead ion from water using banana stem scutcher generated in fiber extraction process. *Results Eng*. 2022;14:100439. doi: 10.1016/j.rineng.2022.100439
8. Suhani N, Saphira M, Mohamed R, *et al*. Removal of COD and ammoniacal Nitrogen by banana trunk fiber with chitosan adsorbent. *Malays J Fundam Appl Sci*. 2020;16:243-247. doi: 10.11113/mjfas.v16n2.1926
9. Fernanda OD, Putri TF, Marfuah S, Aliyatulmuna A, Fajaroh F. Utilization of banana peels extracts in the synthesis of ZnO nanoparticles. *AIP Conf Proc*. 2021;2330:070004. doi: 10.1063/5.0043386
10. Venkatesh AL, Chandralekha D, Bhoomika S, Sreenidhi S, Abhijith GS. Waste water treatment of industrial effluents using banana stem extract. *Int Res J Eng Technol.* 2021;8:357-361.
11. Qasem NAA, Mohammed RH, Lawal DU. Removal of heavy metal ions from wastewater: A comprehensive and critical review. *NPJ Clean Water*. 2021;4(1):36. doi: 10.1038/s41545-021-00127-0
12. Al-Qodah Z, Yahya MA, Al-Shannag M. On the performance of bioadsorption processes for heavy metal ions removal by low-cost agricultural and natural by-products bioadsorbent: A review. *Desalination Water Treat*. 2017;85:339-357. doi: 10.5004/dwt.2017.21256
13. Costa WD, Da Silva Bento AM, De Araújo JAS, *et al*. Removal of copper(II) ions and lead(II) from aqueous solutions using seeds of *Azadirachta indica* A. Juss as bioadsorvent. *Environ Res*. 2020;183:109213. doi: 10.1016/j.envres.2020.109213
14. Burakov AE, Galunin EV, Burakova IV, *et al*. Adsorption of heavy metals on conventional and nanostructured materials for wastewater treatment purposes: A review. *Ecotoxicol Environ Saf*. 2018;148:702-712. doi: 10.1016/j.ecoenv.2017.11.034
15. Awual MR, Hasan MM. Novel conjugate adsorbent for visual detection and removal of toxic lead(II) ions from water. *Microporous Mesoporous Mater*. 2014;196:261-269. doi: 10.1016/j.micromeso.2014.05.021
16. Awual MR. Mesoporous composite material for efficient lead(II) detection and removal from aqueous media. *J Environ Chem Eng*. 2019;7(3):103124. doi: 10.1016/j.jece.2019.103124
17. Tariba Lovaković B. Cadmium, arsenic, and lead: Elements affecting male reproductive health. *Curr Opin Toxicol*. 2020;19:7-14. doi: 10.1016/j.cotox.2019.09.005
18. Shahat A, Hassan HMA, Azzazy HME, El-Sharkawy EA, Abdou HM, Awual MR. Novel hierarchical composite adsorbent for selective lead(II) ions capturing from wastewater samples. *Chem Eng J*. 2018;332:377-386. doi: 10.1016/j.cej.2017.09.040
19. Amin MT, Alazba AA, Amin MN. Absorption behaviours of copper, lead, and arsenic in aqueous solution using date palm fibres and orange peel: Kinetics and thermodynamics. *Pol J Environ Stud*. 2017;26(2):543-557. doi: 10.15244/pjoes/66963
20. Lan Y, Lei X, Zhao C, *et al*. Study on the polypeptide-functionalized magnetic chitosan microspheres that specifically adsorb Hg (II) ions. *Sep Purif Technol*. 2023;323:124386. doi: 10.1016/j.seppur.2023.124386
21. Sousa Neto VO, Oliveira AG, Teixeira RNP, *et al*. Use of coconut bagasse as alternative adsorbent for separation of copper (II) ions from aqueous solutions: Isotherms, kinetics, and thermodynamic studies. *Bioresources*. 2011;6(3):3376-3395. doi: 10.15376/biores.6.3.3376-3395
22. Senthil Kumar P, Ramalingam S, Abhinaya RV, Kirupha SD, Murugesan A, Sivanesan S. Adsorption of metal ions onto the chemically modified agricultural waste. *Clean (Weinh)*. 2012;40(2):188-197. doi: 10.1002/clen.201100118
23. Feng N, Guo X, Liang S, Zhu Y, Liu J. Biosorption of heavy metals from aqueous solutions by chemically modified orange peel. *J Hazard Mater*. 2011;185(1):49-54. doi: 10.1016/j.jhazmat.2010.08.114
24. Giraldo L, Moreno-Piraján JC. Pb2+ adsorption from aqueous solutions on activated carbons obtained from lignocellulosic residues. *Braz J Chem Eng*. 2008;25(1):143-151. doi: 10.1590/S0104-66322008000100015
25. Escudero-Oñate C, Villaescusa I. The thermodynamics of heavy metal sorption onto lignocellulosic biomass. In: *Heavy Metals.* London: IntechOpen; 2018. doi: 10.5772/intechopen.74260
26. Shreya Rajendra U, Rani RA. Wastewater treatment using banana pith powder. *Int J Innov Sci Eng Technol*. 2021;8:622-630.
27. Abdulfatai J, Saka AA, Afolabi AS, Micheal O. Development of adsorbent from banana peel for wastewater treatment. *Appl Mech Mater*. 2013;248:310-315. doi: 10.4028/www.scientific.net/amm.248.310
28. Rizwan S NP, Sheela JS, Prema MK, Gifta CC. Waste water treatment using banana stem extract from textile industries. *Int J Appl Environ Sci*. 2018;13:105-119.
29. Nguyen TT, Thi BTN, Phan PT, *et al*. Synthesis of

microcrystalline cellulose from banana pseudo-stem for adsorption of organics from aqueous solution. *Eng Appl Sci Res*. 2021;48(4):368-378.
doi: 10.14456/easr.2021.39

30. Kusumawardani Y, Subekti S, Astuti W, Soehartono S. Portable wastewater treatment plant using banana stem filter media in small scale motor vehicle washing services. In: *IOP Conf Ser Earth Environ Sci*. 2021;746:012039.
doi: 10.1088/1755-1315/746/1/012039
31. Venkatachalam CD, Govindaraj A, Sengottian M, Ravichandran SR. Recent trends in advanced oxidation processes for tannery effluent treatment - a review. In: *Development in Wastewater Treatment Research and Processes: Advanced Oxidation Processes for Tannery Effluent*. Netherlands: Elsevier; 2024. p. 75-87.
doi: 10.1016/B978-0-323-95656-7.00006-3
32. Alwi H, Idris J, Musa M, Ku Hamid KH. A preliminary study of banana stem juice as a plant-based coagulant for treatment of spent coolant wastewater. *J Chem*. 2013;2013:165057.
doi: 10.1155/2013/165057
33. Subagyo A, Chafidz A. *Banana Pseudo-Stem Fiber: Preparation, Characteristics, and Applications*. 2018.
doi: 10.5772/intechopen.82204
34. Kani KM, Gopika GL. Accessing the suitability of using banana pith juice as a natural coagulant for textile wastewater treatment. *Int J Sci Eng Res*. 2016;7(4):260-264.
35. Kusumawardani Y, Soehartono S, Subekti S. The effectiveness of reducing COD, TSS, and detergent using banana stem filter media in the wastewater treatment of motor vehicles waste treatment. *J Pres Media Komunikasi Pengembangan Teknik Lingkungan*. 2021;18(1):37-44.
doi: 10.14710/presipitasi.v18i1.37-44
36. Mokhtar NM, Priyatharishini M, Kristanti RA. Study on the effectiveness of banana peel coagulant in turbidity reduction of synthetic wastewater. *Int J Eng Technol Sci*. 2019;6(1):82-90.
doi: 10.15282/ijets.v6i1.2109
37. Matsedisho B, Otieno B, Kabuba J, Leswifi T, Ochieng A. Removal of Ni(II) from aqueous solution using chemically modified cellulose nanofibers derived from orange peels. *Int J Environ Sci Technol*. 2024;22:2905-2916.
doi: 10.1007/s13762-024-05819-x
38. Ramu S. *Treatment of Wastewater Using Banana and Lemon Peels as Adsorbents*; 2017. Available from: https://www.researchgate.net/publication/323473059 [Last accessed on 2025 Jun 30].
39. Harshananda TN, Ayisha TM, Priyanka PR, Dildar Mather KN, Vijayakumar R. Removal of colour from textile effluent by adsorption using banana stem and coffee husk: A review. *IOSR J Mech Civil Eng*. 2020;17(4):32-41.
doi: 10.9790/1684-1704013241
40. Pawar S, Bagali S, Uma K, Gowrishankar BS. Column study using modified banana pseudo stem as adsorbent for removal of Pb (II). *Heliyon*. 2023;9(5):e15469.
doi: 10.1016/j.heliyon.2023.e15469
41. Rahman MW, Nipa ST, Rima SZ, *et al*. Pseudo-stem banana fiber as a potential low-cost adsorbent to remove methylene blue from synthetic wastewater. *Appl Water Sci*. 2022;12(10):242.
doi: 10.1007/s13201-022-01769-2
42. Annadurai G, Juang RS, Lee DJ. Adsorption of heavy metals from water using banana and orange peels. *Water Sci Technol*. 2002;47:185-190.
43. Fernandez ME, Nunell GV, Bonelli PR, Cukierman AL. Activated carbon developed from orange peels: Batch and dynamic competitive adsorption of basic dyes. *Ind Crops Prod*. 2014;62:437-445.
doi: 10.1016/j.indcrop.2014.09.015
44. Gupta VK, Ali I. Removal of lead and chromium from wastewater using bagasse fly ash - a sugar industry waste. *J Colloid Interface Sci*. 2004;271(2):321-328.
doi: 10.1016/j.jcis.2003.11.007